Highly Efficient Induction of Chirality in Intramolecular [2 + 2] Cycloadditions between Ketenimines and Imines

Fernando P. Cossío* and Ana Arrieta

Kimika Fakultatea, Euskal Herriko Unibertsitatea, P. K. 1072, 20080 San Sebastián-Donostia, Spain

Begoña Lecea

Farmazi Fakultatea, Euskal Herriko Unibertsitatea, P. K. 450, 01080 Vitoria-Gasteiz, Spain

Mateo Alajarín,* Angel Vidal, and Fulgencio Tovar

Departamento de Química Orgánica, Facultad de Química,Campus de Espinardo, Universidad de Murcia, 30100 Murcia, Spain

Received November 29, 1999

Highly stereocontrolled, intramolecular [2 + 2] cycloadditions between ketenimines and imines leading to 1,2-dihydroazeto[2,1-*b*]quinazolines have been achieved. The source of stereocontrol is a chiral carbon atom adjacent either to the iminic carbon or nitrogen atom. In the first case, the stereocontrol stems from the preference for the axial conformer in the first transition structure. In the second case, the origin of the stereocontrol lies on the two-electron stabilizing interaction between the C−C bond being formed and the σ^* orbital corresponding to the polar C−X bond, X being an electronegative atom. These models can be extended to other related systems for predicting the stereochemical outcome in this intramolecular reaction.

Introduction

Whereas the participation of ketenimines in [4 + 2] cycloaddition reactions, where these heterocumulenes can play the role of either the 2- or 4-atom component, is well documented,[1] [2 + 2] cycloadditions in which the ketenimine function is directly involved as one of the reacting partners are considerably less common.[2] Closely related to these last processes, [2 + 2] cycloadditions of keteniminium cations with imines have been successfully applied in the field of β-lactam synthesis.[3] By contrast, the analogous reaction of ketenimines with imines to furnish azetidin-2-imines has received limited attention, taking place intermolecularly only if the electrophilic character of the ketenimine is enhanced by the presence of electron-withdrawing substituents (such as tosyl[4] or cyano[5]) on the nitrogen atom of the ketenimine function. Additionally, these *intermolecular* [2 + 2] cycloadditions of ketenimines with imines, in the few examples reported, have shown erratic degrees of diastereoselectivity at the 3,4-positions of the four-membered products.[4,5]

As result of our studies on the chemistry of ketenimines, we recently described the first examples of entropically assisted *intramolecular* [2 + 2] cycloadditions of ketenimines with imines,[6] starting from the iminoketenimines of general structure **1**, which led to the previously unknown azeto[2,1-*b*]quinazolines **2** (n = 1) and azeto[2,1-*b*][1,3]benzodiazepines **2** (n = 2).

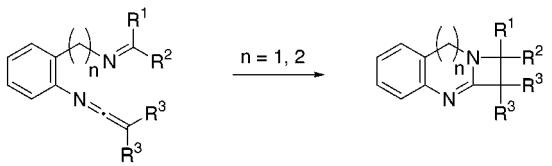

1 **2**

Recently, we reported a highly diastereoselective version of these model reactions on the basis of the desymmetrization of the ketenimine fragment by placing two different substituents on its sp^2 carbon terminus, thus making its two faces enantiotopic. The combination with an imine fragment of similar topicity gave rise to azeto[2,1-*b*]quinazolines **3** containing two stereogenic carbon

(1) Ketenimines as two-atom components in [4 + 2] cycloadditions: (a) Barbaro, G.; Battaglia, A.; Giorgianni, P. *J. Org. Chem.* **1988**, *53*, 5501. (b) Molina, P.; Alajarín, M.; Vidal, A. *Tetrahedron Lett.* **1991**, *32*, 5379. (c) Molina, P.; Alajarín, M.; Vidal, A. *J. Org. Chem.* **1992**, *57*, 6703. (d) Kee-Jung, L.; Heung-Taeck, K.; Boo-Geun, K. *J. Heterocycl. Chem.* **1997**, *34*, 1795. Ketenimines as four-atom components in [4 + 2] cycloadditions: (e) Ghosez, L.; de Pérez, C. *Angew. Chem., Int. Ed. Engl.* **1971**, *10*, 184. (f) Sonveaux, E.; Ghosez, L. *J. Am. Chem. Soc.* **1973**, *95*, 5417. (g) Dondoni, A. *Heterocycles* **1980**, *14*, 1547. (h) Differding, E.; Ghosez, L. *Tetrahedron Lett.* **1985**, *26*, 1647. (i) Differding, E.; Vandevelde, O.; Roekens, B.; Trieu, T.; Ghosez, L. *Tetrahedron Lett.* **1987**, *28*, 397. (j) Molina, P.; López-Leonardo, C. *Tetrahedron Lett.* **1993**, *34*, 2809. (k) Molina, P.; López-Leonardo, C.; Alcántara, J. *Tetrahedron* **1994**, *50*, 5027. (l) Andrews, I. P.; Bannister, R.; Etridge, S. K.; Lewis, N. J.; Mullane, M. V.; Wells, A. S. *Tetrahedron Lett.* **1995**, *36*, 7743. (m) Kee-Jung, L.; Seong-Heon, K.; Jong-Hyuk, K. *Synthesis* **1997**, 1461. (n) Barluenga, J.; Ferrero, M.; Palacios, F. *Tetrahedron* **1997**, *53*, 4521. (o) Alajarín, M.; Vidal, A.; Tovar, F.; Conesa, C. *Tetrahedron Lett.* **1999**, *40*, 6127. For a review on pericyclic reactions of ketenimines, see: Alajarín, M.; Vidal, A.; Tovar, F. *Targets Heterocycl. Syst.* Manuscript in preparation.

(2) (a) Ulrich, H. *Cycloaddition Reactions of Heterocumulenes*; Academic Press: New York, 1967. (b) Patai, S. *The Chemistry of Ketenes, Allenes and Related Compounds*; Wiley: New York, 1980.

(3) (a) Ghosez, L.; Marchand-Brynaert, J. *Comprehensive Organic Synthesis*; Trost, B. M., Fleming, I., Eds.; Pergamon Press: Oxford, 1991; Vol. 5, pp 108−113. (b) Belzecki, C.; Rogalska, E. *J. Chem. Soc., Chem. Commun.* **1981**, 57. (c) Ghosez, L.; Bogdan, S.; Ceresiat, M.; Frydrych, C.; Marchand-Brynaert, J.; Moya-Portuguez, M.; Huber, I. *Pure Appl. Chem.* **1987**, *59*, 393.

(4) Van Camp, A.; Goossens, D.; Moya-Portuguez, M.; Marchand-Brynaert, J.; Ghosez, L. *Tetrahedron Lett.* **1980**, *21*, 3081.

(5) Arnold, B.; Regitz, M. *Angew. Chem., Int. Ed. Engl.* **1979**, *18*, 320.

(6) (a) Alajarín, M.; Molina, P.; Vidal, A. *Tetrahedron Lett.* **1996**, *37*, 8945. (b) Alajarín, M.; Molina, P.; Vidal, A.; Tovar, F. *Tetrahedron* **1997**, *53*, 13449.

10.1021/jo991826q CCC: $19.00
Published on Web 05/18/2000

Scheme 1[a]

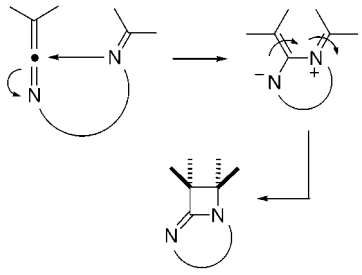

[a] The substituents at the different positions are not specified.

atoms, C1 and C2, with the formation of a clear excess of the cis diastereoisomer over the trans.[7]

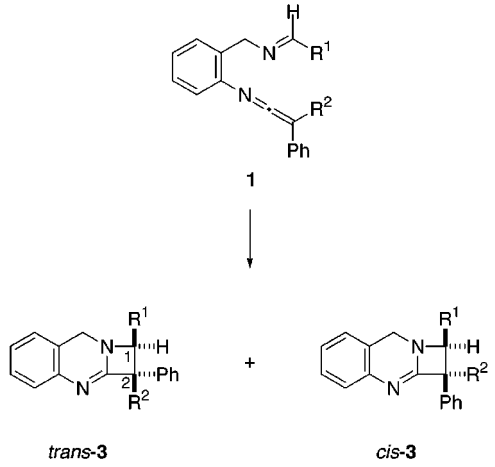

In parallel to these experimental findings, we have performed theoretical studies in order to understand the mechanism of these transformations and to elucidate the main variables that govern its stereochemical outcome. In a previous study,[7] we have found that the reaction between neutral ketenimines and imines does not take place via concerted mechanisms, but consists of a stepwise process (Scheme 1). In a first step, the nitrogen lone pair of the imine adds to the sp-hybridized carbon atom of the ketenimine. The resulting zwitterionic intermediate is transformed into the corresponding azetidin-2-imine via a conrotatory thermal ring closure. This mechanism is qualitatively similar to the well-known Staudinger reaction between ketenes and imines. However, in this latter reaction the limiting step is the second one, in which the two new chiral centers are formed.[8] Instead, the energetic balance in the reaction between ketenimines and imines is more complex. In this reaction the stereocontrol is actually transferred to the first step, thus allowing remarkable levels of stereoselectivity even when the torquoelectronic effects operating in the second step are canceled.

As a further step in the study of the intramolecular [2 + 2] cycloaddition of ketenimines with imines, we have devoted considerable efforts to find out appropriate ways for inducing chirality into this reaction. Ideally there are three sites on the iminoketenimines of general structure **1** where a chiral stereocenter may be located: (a) the amine component of the imine, which is the carbon atom/s linking the aromatic nucleus to the iminic nitrogen atom; (b) the carbonyl component of the imine, which is the substituents on the iminic carbon; and (c) the ketene precursor of the ketenimine, which is the substituents on the carbon atom of the ketenimine fragment.

Herein, we report the results obtained in the study of the intramolecular [2 + 2] cycloaddition of ketenimines with imines when amines or aldehydes with an asymmetric center were used to prepare the imine fragment, cases (a) and (b) above. In addition, as we did in our previous paper,[7] we have performed a computational study in order to understand the reasons underlying the stereocontrol experimentally observed.

Results and Discussion

Chiral Imines Derived from Chiral Amines. Reaction of the racemic chiral amines 1-(*o*-azidophenyl)-ethylamine **4a** and 2-azido-α-phenylbenzylamine **4b** with aromatic, heteroaromatic, α,*β*-unsaturated, or aliphatic aldehydes in the presence of anhydrous magnesium sulfate[9] or basic alumina[10] gave rise to the corresponding aldimines **5** in almost quantitative yields. Azidoimines **5** were generally used in the next reaction step as crude products due to the partial hydrolytic cleavage of the imino bond during purification attempts by crystallization or column chromatography. In all cases, ^{1}H and ^{13}C NMR data of **5** showed only one set of signals, which we have associated with the unique formation of the aldimines with *E* configuration of the imino C═N bond.[6a] When crude azidoimines **5** were treated with a 1 M toluene solution of trimethylphosphane, evolution of dinitrogen was clearly observed indicating their conversion into the corresponding trimethylphosphazenes **6**.[11] These compounds were not isolated but treated in the same reaction flask with an equivalent amount of diphenylketene. IR spectra of small aliquots of the resulting reaction mixtures showed strong absorptions around 2000 cm^{-1}, attributable to the C═C═N grouping of iminoketenimines **7**, which resulted from an aza-Wittig reaction[12] of the phosphazene with the ketene. After some hours in solution at room temperature, iminoketenimines **7** converted into the corresponding azeto[2,1-*b*]quinazolines **8** through a formal intramolecular [2 + 2] cycloaddition between the imino C═N and the cumulated C═C bonds (Scheme 2). Compounds **8** were obtained in moderate to good yields after purification by column chromatography (Table 1) and were characterized by their analytical and spectral data, which were essentially similar to those of compounds **2** and **3** reported previously.[6,7]

These intramolecular [2 + 2] reactions of the iminoketenimines **7**, which present an imino fragment with diastereotopic faces due to the chiral center on the amine component, yielded compounds **8** containing a new stereogenic carbon atom C1, in a highly diastereoselective manner, with a clear excess of the trans diastereoisomer

(7) Alajarín, M.; Vidal, A.; Tovar, F.; Arrieta, A.; Lecea, B.; Cossío, F. P. *Chem. Eur. J.* **1999**, *5*, 1106.

(8) (a) Cossío, F. P.; Arrieta, A.; Lecea, B.; Ugalde, J. M. *J. Am. Chem. Soc.* **1994**, *116*, 2085. (b) Assfeld, X.; Sordo, T. L.; Sordo, J. A.; Gonzalez, J. *J. Org. Chem.* **1993**, *58*, 7036.

(9) Tamura, O.; Hashimoto, M.; Kobayashi, Y.; Katoh, T.; Nakatani, K.; Kamada, M.; Hayakawa, I.; Akiba, T.; Tesashima, S. *Tetrahedron Lett.* **1992**, *33*, 3483.

(10) Texier-Boullet, F. *Synthesis* **1985**, 679.

(11) (a) Gololobov, Y. G.; Zhmurova, I. N.; Kasukhin, L. F. *Tetrahedron* **1981**, *37*, 437. (b) Gololobov, Y. G.; Kasukhin. L. F. *Tetrahedron* **1992**, *48*, 1353.

(12) (a) Eguchi, S.; Matsushita, Y.; Yamashita, K. *Org. Prep. Proced. Int.* **1992**, *24*, 209. (b) Molina, P.; Vilaplana, M. J. *Synthesis* **1994**, 1197.

Scheme 2[a,b]

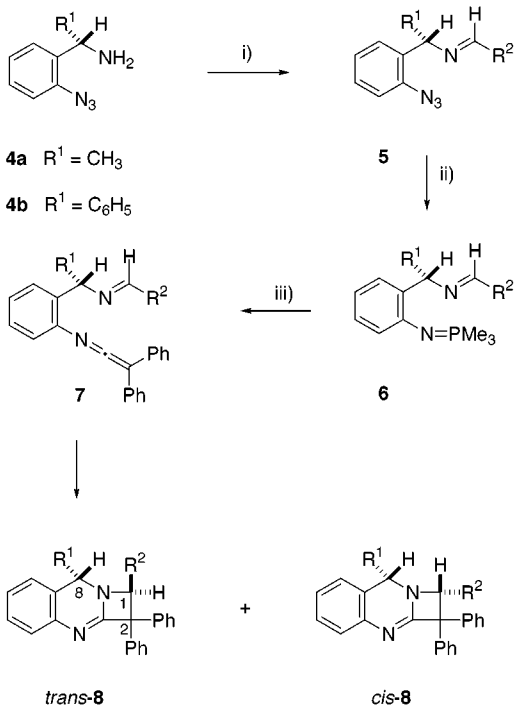

[a] Key: (i) method A: R^2-CHO, Et_2O, anhyd $MgSO_4$, 25 °C, 12 h; method B: R^2-CHO, basic Al_2O_3, 25 °C, 12 h; (ii) PMe_3, toluene, 25 °C, 30 min; (iii) $Ph_2C{=}C{=}O$, toluene, 25 °C, 1 h. [b]Only one enantiomer is drawn for each compound.

Table 1. Azeto[2,1-*b*]quinazolines 8 and 9

compd	R^1	R^2	cis/trans[a]	yield[b] (%)
8a	CH_3	4-O_2N-C_6H_4	11:89	82
8b	CH_3	4-CH_3O-C_6H_4	4:96	68
8c	CH_3	1-naphthyl	<2:98	65
8d	CH_3	3-thienyl	6:94	63
8e	CH_3	(*E*)-C_6H_5-CH=CH	<2:98	78
8f	CH_3	(*E*)-2-O_2N-C_6H_4-CH=CH	<2:98	58
8g	CH_3	$(CH_3)_2CH$	17:83	67
8h	CH_3	$(CH_3)_3C$	23:77	43
8i	C_6H_5	4-O_2N-C_6H_4	9:91	80
8j	C_6H_5	4-H_3C-C_6H_4	10:90	50
8k	C_6H_5	$(CH_3)_2CH$	27:73	66
9a	CH_3	4-O_2N-C_6H_4	<2:98	62
9b	CH_3	$(CH_3)_2CH$	20:80	26
9c	C_6H_5	4-O_2N-C_6H_4	<2:98	62
9d	C_6H_5	4-H_3C-C_6H_4	4:96	50
9e	C_6H_5	$(CH_3)_2CH$	15:85	37

[a] As determined by ^{1}H NMR (300 MHz) analysis of the crude reaction mixtures. [b] Yield of pure isolated major diastereoisomer.

over the cis (Table 1), thus showing the high stereocontrol exerted by the R^1 substituent on the benzylic carbon over the configuration of the new chiral center. Higher diastereoisomeric excesses were obtained from imine fragments derived from aromatic, heteroaromatic, or α,β-unsaturated aldehydes (compounds **8a**−**f**,**i**,**j**) than from aliphatic ones (**8g**,**h**,**k**). Only minor differences were found by the employment of the α-CH_3 or α-Ph substituents on the preexisting chiral center (compare cis/trans ratios of **8a** vs **8i** and **8g** vs **8k**).

The ratio of isomers was calculated by integration of the signals due to H1, H8, and/or C*H*$_3$-C8 in the ^{1}H NMR (300 MHz) spectra of the crude reaction mixtures, before the purification step. In the reactions that yielded mixtures of diastereoisomers, the major one could be separated in a pure form by column chromatography.

Table 2. Selected ^{1}H NMR Data of Azeto[2,1-*b*]quinazolines 8

	δ H1 (ppm)		δ H8 (ppm)		δ C*H*$_3$−C8 (ppm)	
compd	*trans*-**8**	*cis*-**8**	*trans*-**8**	*cis*-**8**	*trans*-**8**	*cis*-**8**
8a	5.86	5.54	4.73	4.83	1.42	1.30
8b	5.68	5.38	4.72	4.82	1.40	1.20
8c	6.49	a	4.87	a	1.54	a
8d	5.80	5.52	4.76	4.82	1.42	1.32
8e	5.23	*a*	4.80	*a*	1.45	*a*
8f	5.31	*a*	4.86	*a*	1.48	*a*
8g	4.35	4.31	4.79	4.68	1.30	1.63
8h	4.63	4.55	4.72	4.74	1.27	1.70
8i	5.36	5.59	5.58	5.72		
8j	5.24	5.47	5.60	5.70		
8k	3.92	4.29	5.63	5.60		

[a] Diastereoisomers not obtained in this work.

Only in one case, **8h**, both isomers were separated and characterized as such (see the Experimental Section).

The cis/trans configuration of the diastereoisomeric reaction products was assigned on the basis of their ^{1}H NMR data and by nuclear Overhauser (NOE) experiments. Irradiation of the signal at δ 1.42 ppm corresponding to the hydrogens of the methyl group C*H*$_3$-C8 in the major isomer of compound **8a** (R^1 = CH_3, R^2 = 4-O_2N-C_6H_4) induced a 10.9% enhancement of the H1 signal (δ 5.86 ppm), whereas NOE enhancement could not be observed on the H1 signal when the H8 proton (δ 4.73 ppm) was irradiated. These results evidence that the major isomer formed in the [2 + 2] cycloaddition here reported is the one with the hydrogens H1 and H8 in a trans relative configuration, *trans*-**8a**. Similar outcomes were obtained on the major isomers of the rest of compounds **8**. Moreover, the comparison of the chemical shifts of the H8 and C*H*$_3$-C8 protons in the ^{1}H NMR spectra of the major and minor isomers of the azetoquinazolines **8** bearing an aryl, heteroaryl, or vinyl substituent at C1 (compounds **8a**−**f**,**i**,**j**) serves to ascertain the configurational assignment made above (Table 2). The trans isomers show the H8 proton shifted upfield, when compared with the cis, due probably to the magnetic shielding exerted by the nearby aryl, heteroaryl, or vinyl group at C1, in a relative cis position. A similar anisotropic effect can explain the differences observed in the chemical shifts of the C*H*$_3$-C8 protons between both isomers in compounds **8a**−**d**, as well the shielding of the H1 proton in the trans isomers of compounds **8i**−**k**, in this last case due to the phenyl group at C8 in a relative cis position to this proton.

In a previous work we have shown that trimethylsilylketene could be used as efficiently as diphenylketene in a reaction sequence similar to the one reported in Scheme 2, giving rise to 2-unsubstituted azeto[2,1-*b*]-quinazolines due to protonolysis of the C2-silicon bond during the chromatographic purification (SiO_2 column) of the reaction products.[6b] Sequential treatment of imines **5** with trimethylphosphane and trimethylsilylketene led, after purification by column chromatography, to azetoquinazolines **9** (Scheme 3), unsubstituted at carbon C2, with the same degree and sense of stereocontrol that in the sequence leading to **8**. Similarly to that results, compounds **9** were also obtained with higher degree of diastereoselectivity when the imine fragment derived from aromatic instead of aliphatic aldehydes, and no remarkable differences were observed by changing from α-CH_3 to α-Ph at the benzylic carbon atom (Table 1).

Although in this work we have not carried out reactions

Scheme 3[a,b]

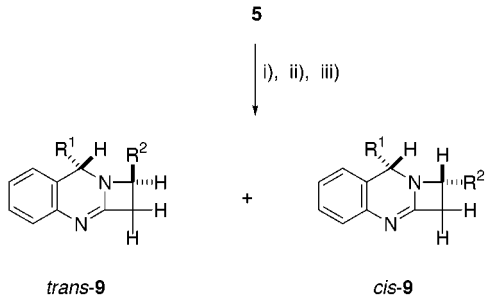

[a] Key: (i) PMe_3, toluene, 25 °C, 30 min; (ii) $Me_3SiCH{=}C{=}O$, toluene, reflux, 2 h; (iii) silica gel. [b]Only one enantiomer is drawn for each compound.

on optically active iminoketenimines type **7**, the easy availability of enantiomerically enriched (*S*)-(−)-1-(*o*-azidophenyl)ethylamine[13] makes the reactions above potentially useful for preparing 1,2-dihydroazeto[2,1-*b*]-quinazolines, such as *trans*-**8** and **9**, in non racemic forms given that the occurrence of racemization in the [2 + 2] cycloadditions seems unlikely.

Chiral Imines Derived from Chiral Aldehydes. As mentioned in the Introduction, a second site to locate a chirality directing group may be the substituents on the iminic carbon atom of the iminoketenimines of general structure **1**. For instance, it has been shown that the Staudinger reaction between ketenes and imines to give *β*-lactams occurs with high stereocontrol if a chiral carbon atom, bearing one heteroatom attached to it, is directly linked to the iminic carbon atom.[14] Due to the apparent similarity between the Staudinger reaction and the [2 + 2] cycloadditions here discussed, it was hoped that one of those chiral substituents on the iminic carbon of **1** would serve to control efficiently the absolute configuration of the C1 carbon atom in the putative products of the intramolecular cycloaddition.

With this aim in mind, iminoketenimine **10** was prepared starting from 2-azidobenzylamine by sequential treatment with commercially available *tert*-butyl (*S*)-(−)-4-formyl-2,2-dimethyl-3-oxazolidinecarboxylate (Garner's aldehyde), trimethylphosphane, and diphenylketene, a methodology analogous to that in Scheme 2. From the intramolecular [2 + 2] cycloaddition of **10** only one diastereoisomeric product **11** could be detected in the crude reaction mixture and conveniently purified by column chromatography and further crystallization (Scheme 4). Its absolute configuration at C1 was set up attending to the observed coupling constant between H1 and the adjacent hydrogen atom on the oxazolidine ring ($^3J_{HH}$ = 9.6 Hz in $CDCl_3$ at 328 K; $^3J_{HH}$ = 9.3 Hz in DMSO-d_6 at 333 K) in its ^{1}H NMR spectra, a value that is in good accordance with the one described in the literature for similarly 4-substituted *β*-lactams possessing the same syn relative configuration between the two adjacent stereocenters.[15] Moreover, in all the [2 + 2] cycloadditions reported to date of ketenes with chiral imines derived from Garner's aldehyde or other closely related 4-formyl oxazolidines, the relative configuration

Scheme 4

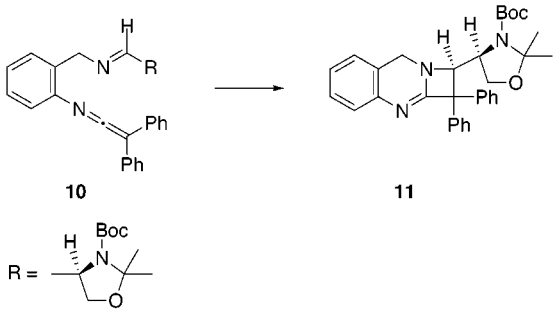

of the C4 and C4′ carbons in the resulting single *β*-lactam stereoisomer has been determined to be syn.[8a,15,16] The same is true for similar Staudinger reactions with imines derived from other chiral α-amino aldehydes.[17]

Computational Studies

Methods. All calculations reported in this paper have been performed using either the GAUSSIAN94[18] or GAUSSIAN98[19] series of programs, with the 3-21G and 6-31G* basis sets.[20] Electron correlation was estimated by means of density functional theory (DFT),[21] in this particular case by using the hybrid method developed by Becke and usually denoted as B3LYP.[22] All the reported stationary points were fully optimized at the HF/3-21G

(13) Molina, P.; Alajarín, M.; Vidal, A. *J. Org. Chem*. **1993**, *58*, 1687.

(14) For some good compilations of references on this theme, see: (a) Georg, G. I.; Ravikumar, V. T. In *The Chemistry of β-Lactams*; Georg, G. I., Ed.; VCH Publishers: New York, 1992; pp 295−368. (b) Jayaraman, M.; Srijaran, V.; Deshmukh, A. R. A. S.; Bhawal, B. M. *Tetrahedron* **1996**, *52*, 3741. (c) ref 8a.

(15) (a) Palomo, C.; Cossío, F. P.; Cuevas, C.; Lecea, B.; Mielgo, A.; Román, P.; Luque, A.; Martínez-Ripoll, M. *J. Am. Chem. Soc.* **1992**, *114*, 9360. (b) Palomo, C.; Cossío, F. P.; Cuevas, C. *Tetrahedron Lett.* **1991**, *32*, 3109. (c) Jayaraman, M.; Deshmukh, A. R., Bhawal; B. M. *Tetrahedron* **1996**, *52*, 8989.

(16) Jayaraman, M.; Nandi, M.; Sathe, K. M.; Deshmukh, A. R. A. S.; Bhawal, B. M. *Tetrahedron*: *Asymmetry* **1993**, *4*, 609.

(17) (a) Palomo, C.; Aizpurua, J. M.; Cuevas, C.; Román, P.; Luque, A.; Martínez-Ripoll, M. *An. Quim. Int. Ed.* **1996**, *92*, 134. (b) Palomo, C.; Aizpurua, J. M.; Cuevas, C.; Urchegui, R.; Linden, A. *J. Org. Chem.* **1996**, *61*, 4400. (c) Palomo, C.; Aizpurua, J. M.; Cabré, F.; García, J. M.; Odriozola, J. M. *Tetrahedron Lett.* **1994**, *35*, 2721. (d) Palomo, C.; Cossío, F. P.; Cuevas, C.; Odriozola, J. M.; Ontoria, J. M. *Tetrahedron Lett.* **1992**, *33*, 4827.

(18) Gaussian 94, Revision B.2: Frisch, M. J.; Trucks, G. W.; Schlegel, H. B.; Gill, P. M. W.; Johnson, B. G.; Robb, M. A.; Cheeseman J. R.; Keith, T.; Petersson, G. A.; Montgomery, J. A.; Raghavachari, K.; Al-Laham, M. A.; Zakrzewski, V. G.; Ortiz, J. V.; Foresman, J. B.; Peng, C. Y.; Ayala, P. Y.; Chen, W.; Wong, M. W.; Andres, J. L.; Replogle, E. S.; Gomperts, R.; Martin, R. L.; Fox, D. J.; Binkley, J. S.; Defrees, D. J.; Baker, J.; Stewart, J. S.; Head-Gordon, M.; Gonzalez, C.; Pople, J. A. Gaussian, Inc., Pittsburgh, PA, 1995.

(19) Gaussian 98, Revision A.5: Frisch, M. J.; Trucks, G. W.; Schlegel, H. B.; Scuseria, G. E.; Robb, M. A.; Cheeseman, J. R.; Zakrzewski, V. G.; Montgomery, Jr., J. A.; Stratmann, R. E.; Burant, J. C.; Dapprich, S.; Millam, J. M.; Daniels, A. D.; Kudin, K. N.; Strain, M. C.; Farkas, O.; Tomasi, J.; Barone, V.; Cossi, M.; Cammi, R.; Mennucci, B.; Pomelli, C.; Adamo, C.; Clifford, S.; Ochterski, J.; Petersson, G. A.; Ayala, P. Y.; Cui, Q.; Morokuma, K.; Malick, D. K.; Rabuck, A. D.; Raghavachari, K.; Foresman, J. B.; Cioslowski, J.; Ortiz, J. V.; Stefanov, B. B.; Liu, G.; Liashenko, A.; Piskorz, P.; Komaromi, I.; Gomperts, R.; Martin, R. L.; Fox, D. J.; Keith, T.; Al-Laham, M. A.; Peng, C. Y.; Nanayakkara, A.; Gonzalez, C.; Challacombe, M.; Gill, P. M. W.; Johnson, B.; Chen, W.; Wong, M. W.; Andres, J. L.; Gonzalez, C.; Head-Gordon, M.; Replogle, E. S.; Pople, J. A. Gaussian, Inc., Pittsburgh, PA, 1998.

(20) Hehre, W. J.; Radom, L.; Schleyer, P. v. R.; Pople, J. A. *Ab Initio Molecular Orbital Theory;* Wiley: New York, 1986; pp 71−82 and references therein.

(21) (a) Parr, R. G.; Yang, W. *Density-Functional Theory of Atoms and Molecules*; Oxford University Press: New York, 1989. (b) Kohn, W.; Becke, A. D.; Parr, R. G. *J. Phys. Chem*. **1996**, *100*, 12974. (c) Bartolott, L. J.; Pluchick, K. In *Reviews in Computational Chemistry*; Lipkowitz, K. B., Boyd, D. B., Eds.; VCH Publishers: New York, 1996; Vol. 7, pp 187−216.

(22) (a) Becke, A. D. *J. Chem. Phys.* **1993**, *98*, 5648. (b) Becke, A. D. *Phys. Rev. A* **1988**, *38*, 3098. (c) Lee, C.; Yang, W.; Parr, R. G. *Phys. Rev. B* **1980**, *37*, 785. (d) Vosko, S. H.; Wilk, L.; Nusair, M. *Can. J. Phys.* **1980**, *58*, 1200.

Scheme 5

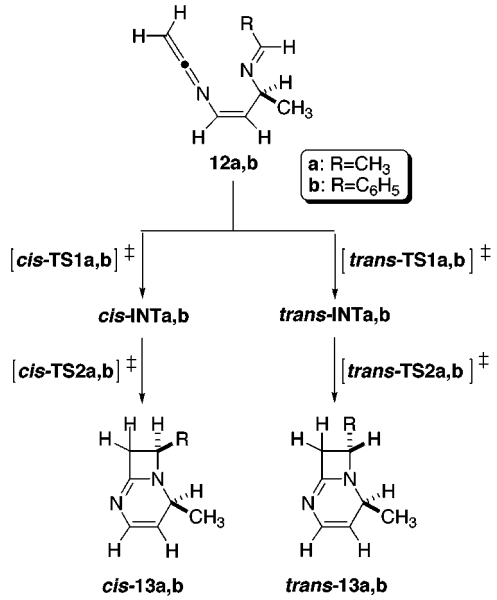

level by analytical gradient techniques and characterized by frequency calculations.[23] Zero-point vibrational energies (ZPVEs) were scaled by 0.89.[24] Solute−solvent interactions were computed by means of the Onsager model,[25] which is denoted here as L1A1.[26] Atomic charges and two-electron interactions were calculated by the natural bond orbital (NBO) method.[27]

Chiral Imines Derived from Chiral Amines. We have selected structures **12a**,**b** as model reactants for the study of the intramolecular [2 + 2] reaction of compounds **7** (R^1 = Me, R^2 = alkyl, aryl, see Scheme 2). In this case, the stereocontrol is dictated by the chiral carbon atom adjacent to the iminic nitrogen, and formation of two diastereomeric 2-iminoazetidines *cis*- and *trans*-**13a**,**b** is possible. We have depicted in Scheme 5 these structures as well as the transition structures and intermediates, which are conceivable from the mechanism previously reported for this reaction.[7]

Assuming that the two substituents of the ketenimine moiety are identical, formation of two diastereomeric reaction intermediates and products is possible, as it is shown in Scheme 6. If we define the ω dihedral angle as indicated in this Scheme, in one zwitterionic intermediate, denoted as **A**, the sign of this dihedral angle is positive. From this intermediate, the conrotatory motion of lowest energy is counterclockwise, since as long as the electrocyclization progresses the ω angle approaches to zero. This conrotation leads to diastereomer **C**. Similarly, the other possible intermediate **B** has a negative value of ω. In this case, clockwise conrotation leads to diastereomer **D**. It is noteworthy that given the (*E*) geometry of the iminic part of the reactant and the substituents of

Scheme 6

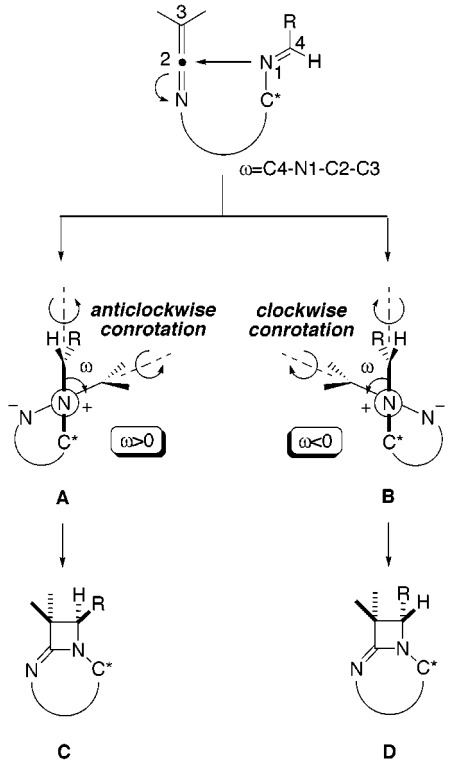

the ketenimine moiety (vide supra), direct interconversion between **A** and **B** is not possible.[8a,28]

Intensive exploration of the corresponding HF/3-21G potential energy surfaces led to the structures depicted in Figures 1−4. Previous work from our laboratory has shown that this theoretical level yields accurate enough geometries.[7] The computed relative energies are reported in Table 3. In this table, the energy differences have been defined according to the reaction profiles depicted in Figure 5.

As we have previously reported,[7] since the concentration of the intermediates is lower than those of the reactants and/or the products, the steady-state approximation can be applied to the computed reaction profiles. Under these conditions, the cis/trans ratio of cycloadducts **13** is given by eq 1

$$\frac{[cis\text{-}\mathbf{13}]}{[trans\text{-}\mathbf{13}]} \approx \frac{\exp[-(\Delta E^{c}_{a1} + \Delta E^{c}_{a2})/RT][\exp(-\Delta E^{t}_{-a1}/RT) + \exp(-\Delta E^{t}_{a2}/RT)]}{\exp[-(\Delta E^{t}_{a1} + \Delta E^{t}_{a2})/RT][\exp(-\Delta E^{c}_{-a1}/RT) + \exp(-\Delta E^{c}_{a2}/RT)]} \quad (1)$$

where

$$\Delta E^{t}_{-a1} = \Delta E^{t}_{a1} - \Delta E^{t}_{int} \quad (2)$$

and

$$\Delta E^{c}_{-a1} = \Delta E^{c}_{a1} - \Delta E^{c}_{int} \quad (3)$$

All magnitudes in eqs 1−3 are reported in Table 3. According to our results, in both the **12a** → **13a** and **12b**

(23) McIver, J. M.; Komornicki, A. K. *J. Am. Chem. Soc.* **1972**, *94*, 2625.

(24) Pople, J. A.; Schleyer, B.; Krishnan, R.; DeFrees, D. J.; Binkley, J. S.; Frish, H.; Whiteside, R.; Hout, R. F., Jr.; Hehre, W. J. *Int. J. Quantum Chem. Symp.* **1981**, *15*, 269.

(25) (a) Onsager, L. *J. Am. Chem. Soc.* **1936**, *58*, 1486. (b) Wong, M. W.; Wiberg, K. B.; Frisch, M. J. *J. Am. Chem. Soc.* **1992**, *114*, 523. (c) Wong, M. W.; Wiberg, K. B.; Frisch, M. J. *J. Am. Chem. Soc.* **1992**, *114*, 1645.

(26) Morao, I.; Lecea, B.; Arrieta, A.; Cossío, F. P. *J. Am. Chem. Soc.* **1997**, *119*, 816.

(27) Reed, A. E.; Curtiss, L. A.; Weinhold, F. *Chem. Rev.* **1988**, *88*, 899.

(28) (a) Dumas, S.; Hegedus, L. S. *J. Org. Chem.* **1994**, *59*, 4967. (b) Hegedus, L. S.; Montgomery, J.; Narukawa, Y.; Snustad, D. C. *J. Am. Chem. Soc.* **1991**, *113*, 5784.

Table 3. Energy Barriers[a,b] (kcal/mol) and Diastereomeric Ratios (cis/trans)[c] Computed for the Reactions Included in Schemes 5 and 7

	ΔE_{a1}		ΔE_{int}		ΔE_{a2}		ΔE_{rxn}		
method	cis (syn)	trans (anti)	cis (syn)	trans (anti)	cis (syn)	trans (anti)	cis (syn)	trans (anti)	cis/ trans (syn/ anti)
				12a → *cis*-**13a** + *trans*-**13a**					
HF/3-21G	28.09	25.67	23.88	21.78	24.98	25.46	−18.95	−19.53	6:94
B3LYP/6-31G*	20.02	17.72	15.07	13.21	13.47	14.26	−20.71	−20.91	14:86
B3LYP(L1A1)/6-31G*[d]	18.94	16.53	13.29	11.75	14.46	14.99	−21.18	−21.34	15:85
				12b → *cis*-**13b** + *trans*-**13b**					
HF/3-21G	32.01	30.11	27.94	26.29	21.61	21.71	−15.78	−16.62	7:93
B3LYP/6-31G*	23.30	21.27	18.66	16.96	8.00	8.68	−17.31	−17.41	15:85
B3LYP(L1A1)/6-31G*[d]	22.64	20.65	17.73	15.81	8.50	9.50	−17.58	−17.71	18:82
				12c → *syn*-**13c** + *anti*-**13c**					
HF/3-21G	27.71	27.23	25.76	24.52	19.11	24.57	−21.09	−17.67	100:0
B3LYP/6-31G*	20.64	20.69	18.57	17.40	6.75	11.66	−19.30	−18.78	100:0
B3LYP(L1A1)/6-31G*[d]	19.93	20.23	17.80	17.51	7.66	11.50	−19.07	−18.46	100:0

[a] See Figures 5 and 9 for the notation of these energy differences. [b] Single-point energies computed from HF/3-21G geometries. The scaled ZPVE corrections have been included. [c] Calculated from eqs 1−3. [d] Values obtained in simulated toluene solution ($\epsilon = 2.38$).

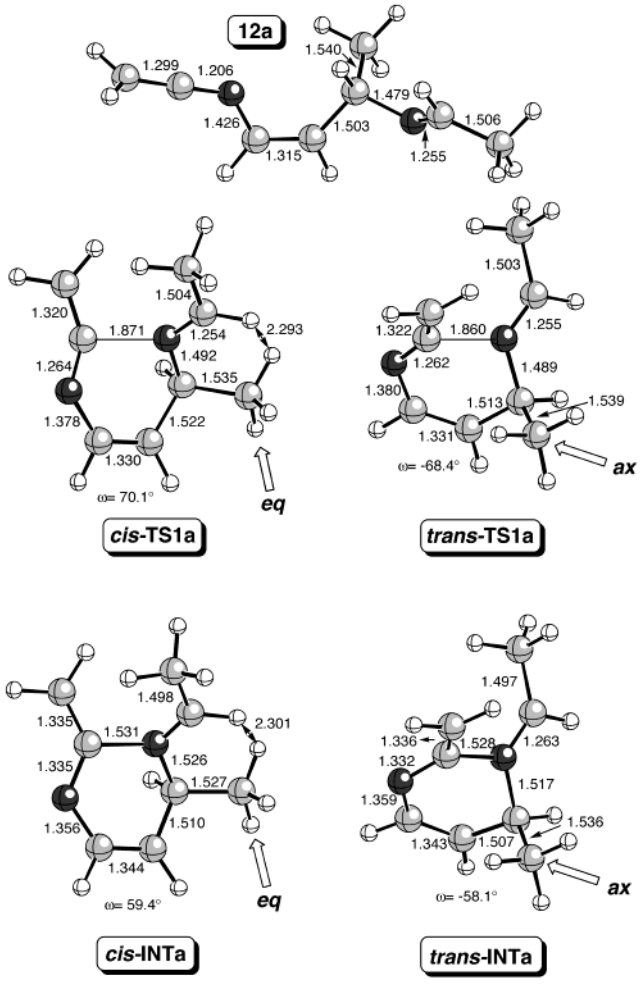

Figure 1. Main geometric features of the stationary points **12a**, *cis*-**TS1a**, *trans*-**TS1a**, *cis*-**INTa**, and *trans*-**INTa** found in the first step of the reaction of **12a** to form *cis*- and *trans*-**13a** (see Scheme 5), computed in the gas phase. Bond distances are given in angstroms and angles in degrees. In this and the following figures which incorporate ball-and-stick drawings, atoms are represented by increasing order of shadowing as follows: H, C, O, N.

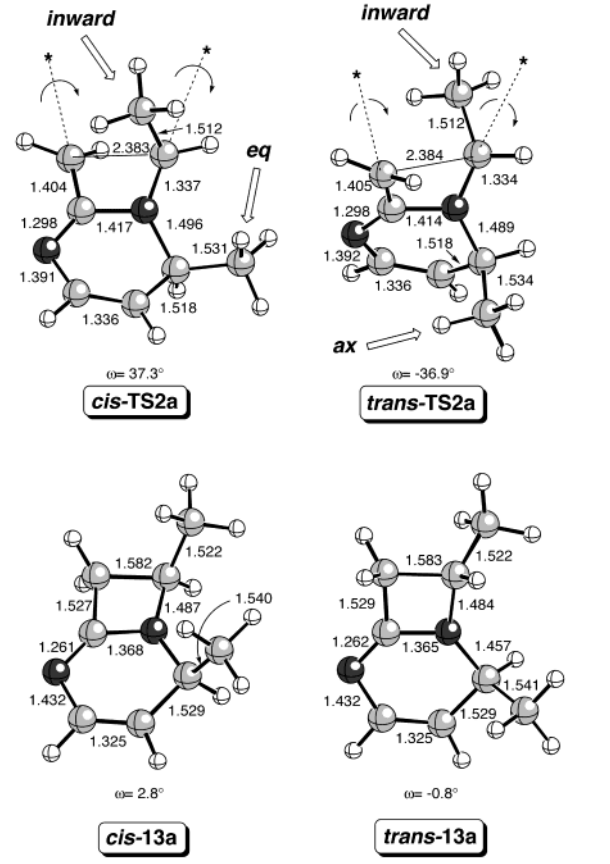

Figure 2. Main geometric features of the stationary points *cis*-**TS2a**, *trans*-**TS2a**, *cis*-**13a**, and *trans*-1**3a** found in the second step of the reaction of **12a** to form *cis*- and *trans*-**13a** (see Scheme 5), computed in the gas phase. See Figure 1 caption for additional details.

→ **13b** transformations the first step is of higher activation energy than the second one. This first step consists of the nucleophilic attack of the nitrogen atom of the imine part of **12a**,**b** on the sp-hybridized carbon atom of the ketenimine (Figures 1 and 3). In this step, a six-membered ring is formed. This new ring is in a half-chair conformation, the methyl groups occupying axial or equatorial positions. For instance, in both *cis*-**TS1a** and *cis*-**INTa** the ω values are positive and the noniminic methyl group is equatorial. This leads to a destabilizing interaction between this group and the hydrogen atom attached to the iminic carbon (Figure 1). In both *trans*-**TS1a** and *trans*-**INTa**, the noniminic methyl group occupies the axial position and therefore this destabilizing interaction is not present. Consequently, the cis stationary points are of higher energy than their trans

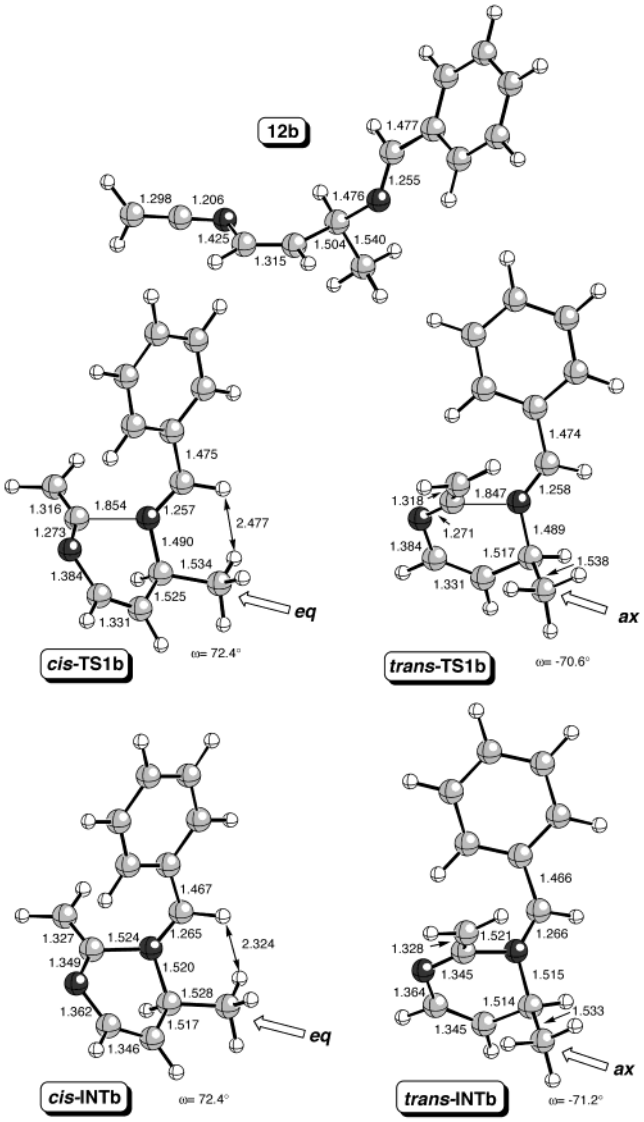

Figure 3. Main geometric features of the stationary points **12b**, *cis*-**TS1b**, *trans*-**TS1b**, *cis*-**INTb**, and *trans*-**INTb** found in the first step of the reaction of **12b** to form *cis*- and *trans*-**13b** (see Scheme 5), computed in the gas phase. See Figure 1 caption for additional details.

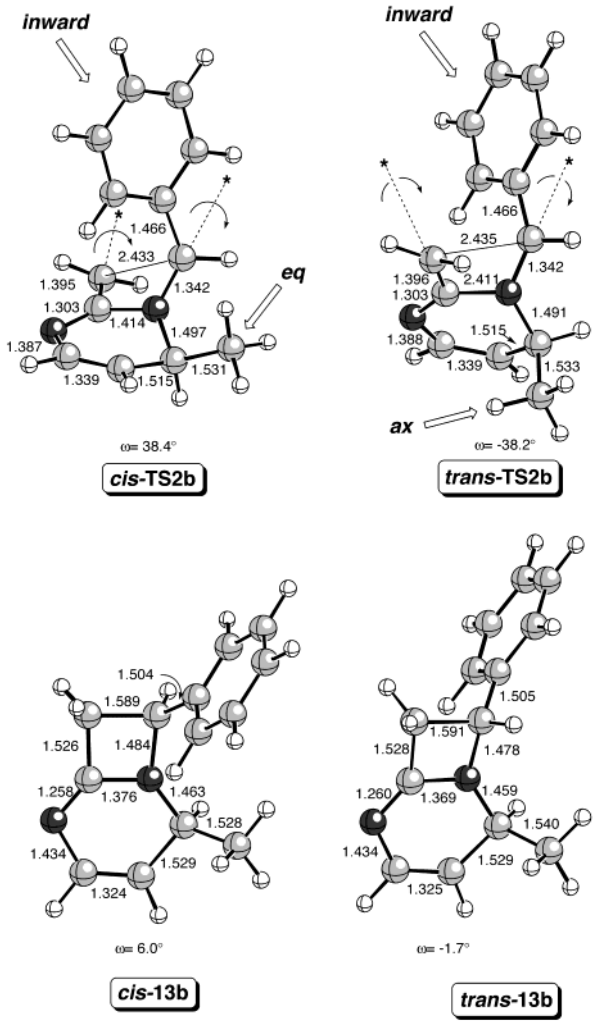

Figure 4. Main geometric features of the stationary points *cis*-**TS2b**, *trans*-**TS2b**, *cis*-**13b**, and *trans*-1**3b** found in the second step of the reaction of **12b** to form *cis*- and *trans*-**13b** (see Scheme 5), computed in the gas phase. See Figure 1 caption for additional details.

analogues. The same analysis can be extended to **TS1b** and **INTb** (see Figure 3).

Counterclockwise conrotation from *cis*-**INTa**,**b** (from the position indicated by an asterisk in Figures 2 and 4) leads to *cis*-**13a**,**b**, *cis*-**TS2a**,**b** being the respective transition structures. Similarly, clockwise conrotation of *trans*-**INTa**,**b** leads to *trans*-**13a**,**b** via *trans*-**TS2a**,**b**. In all these second transition structures the substituents at the iminic carbon atoms occupy the inward position, and therefore, the torquoelectronic effects are similar for the corresponding diastereomeric pairs. In addition, the already formed six-membered rings are more planar as long as the second step proceeds. Therefore, the energy barriers associated with these second steps are quite similar, as is shown by the ΔE_{a2} data reported in Table 3.

In summary, in these transformations the stereocontrol of the whole reaction lies in the first step, namely in the formation of the N1−C2 bond. Applying eq 1, the trans-cycloadducts must be the major reaction products under kinetic control. In addition, the quantitative evaluations of the cis/trans ratios reported in Table 3 compare very well with similar examples reported in Table 1 (compounds **8a**−**h** and **9a**,**b**).

In essence, our model predicts that in these reactions the source of the stereocontrol lies in the proximity between the group present at the chiral methine carbon contiguous to the ortho-disubstituted phenyl ring and the hydrogen atom attached to the iminic carbon. The major isomer is the one that minimizes this proximity occupying an axial position during the first step of the reaction. If this model is correct, a trisubstituted iminic part derived from a ketone should induce even larger diastereoselection.

Chiral Imines Derived from Chiral Aldehydes. We have selected structure **12c** as a model for compound **10**, in which the imine moiety is generated from Garner's aldehyde. The possible stationary points are shown in Scheme 7, and their chief geometric features at HF/3-21G level are reported in Figures 6 and 7. Given the relative flexibility of these structures, several different conformations were checked. In particular, the possible rotamers of the formamide moiety were computed. The structures reported and discussed are those found to be the lowest energy conformers.

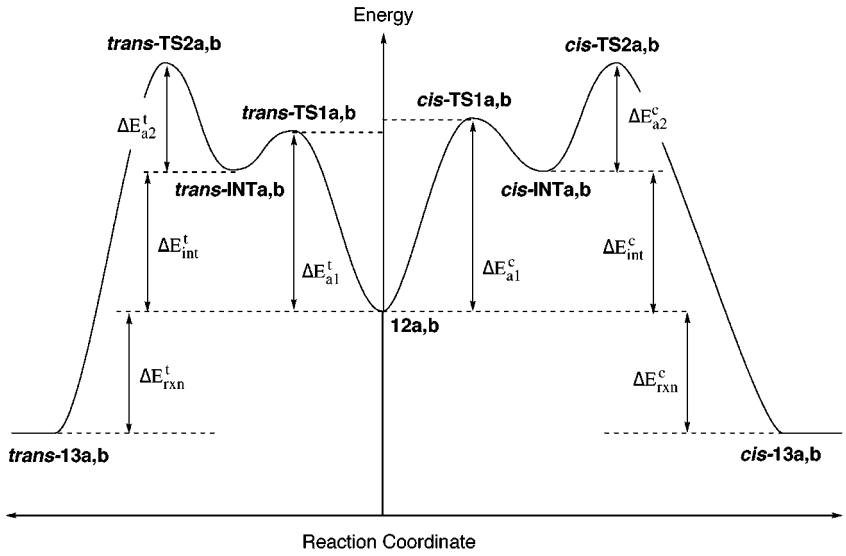

Figure 5. Reaction profile found for the **12a,b** → *cis*-/*trans*-**13a,b** transformation.

Scheme 7

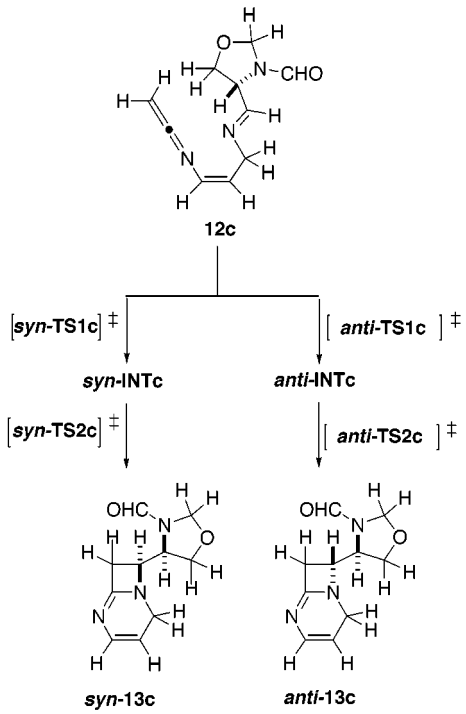

The general features of the first transition structures and the reaction intermediates are similar to those found for the two previous model reactions. In particular, the six-membered ring has a half-chair conformation. However, given that there is one methylene group instead of a chiral methine carbon atom, the energies of both first transition structures and intermediates are quite similar, as can be seen from the ΔE_{a1} and ΔE_{int} data reported in Table 3.

In contrast, the second transition structures are of quite different energies, *syn*-**TS2c** saddle point being ca. 4 kcal/mol more stable than *anti*-**TS2c**. As we have found in previous computational work on the Staudinger reaction between ketenes and imines,[8a] the reason for this significant difference in energy lies in the two-electron interaction between the C1···C2 bond being formed and either the σ^* orbitals located on the C−N or C−C bond of the chiral oxazolidine moiety. Thus, the NBO analysis at the B3LYP/6-31G* level shows that in *syn*-**TS2c** there is a strong stabilizing interaction between the σ(C1···C2) bond being formed and the σ^*(C−N) bond located on the chiral *N*-formyloxazolidine ring, as it is depicted in Figure 8. The second-order perturbation energy associated with this interaction is −12.93 kcal/mol.

This large value is due to the favorable steric environment imposed by the conrotatory geometry of the transition structure and the chirality of the center already present. In particular, the arrangement between C2 and C* is almost linear, thus allowing an efficient overlap (see Figure 8). In contrast, in *anti*-**TS2c** the unfavorable matching between the azetidine ring being formed and the oxazolidine ring does not allow an antiperiplanar arrangement between the C1···C2 and C*−N bonds. Therefore, the C−C bond of the oxazolidine must occupy the antiperiplanar position. However, given that the C−N bond is a better σ-acceptor than the C−C bond, the σ^*-(C−C) NBO is of higher energy than σ^*(C−N), and therefore, the second-order perturbation energy associated with the σ(C1···C2) → σ^*(C−C) is ca. 5.4 kcal lower than that corresponding to the σ(C1···C2) → σ^*(C−N) donation (Figure 8). As a consequence, *anti*-**TS2c** is of higher energy than its syn analogue. From the syn/anti ratio calculated from eq 1 (see Table 3), exclusive formation of syn-**13c** is predicted, in excellent agreement with our experimental finding.

Therefore, the origin of the chiral control in the **12c** → *syn*-**13c** transformation lies in the second step of the reaction as it is shown in the reaction profile depicted in Figure 9. This result is in line with those obtained in more conventional Staudinger reactions between ketenes and imines and contrasts with that previously found for the **12a**,**b** → **13a**,**b** transformations (vide supra).

Conclusions

In the present work, we have shown two ways for inducing chirality at the C1 carbon atom of 1,2-dihydroazeto[2,1-*b*]quinazolines, as obtained in the intramolecular [2 + 2] cycloadditions between ketenimine and imine fragments placed on an ortho-benzylic scaffolding. In the first one, the stereochemical outcome is controlled

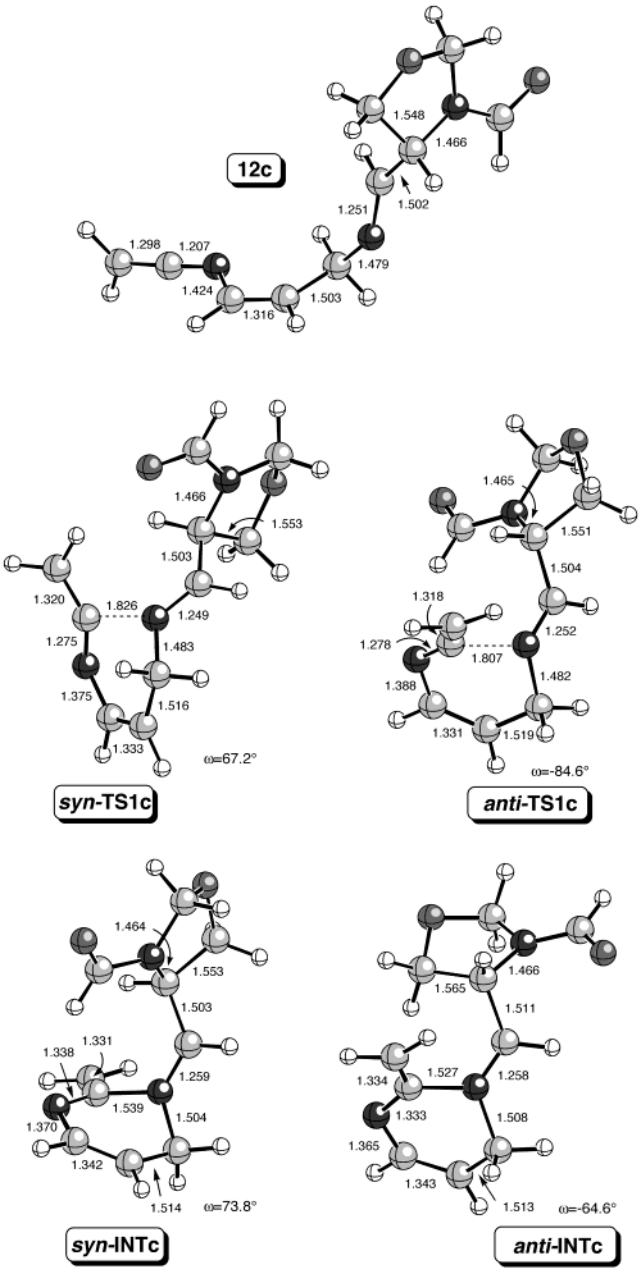

Figure 6. Main geometric features of the stationary points **12c**, *syn*-**TS1c**, *anti*-**TS1c**, *syn*-**INTc**, and *anti*-**INTc** found in the first step of the reaction of **12c** to form *syn*- and *anti*-**13c** (see Scheme 7), computed in the gas phase. See Figure 1 caption for additional details.

by a chiral benzylic carbon adjacent to the iminic nitrogen atom, at two bonds of distance from the new stereogenic center. The second one relies on the stereocontrol exerted by a chiral carbon atom directly linked to the iminic carbon, the future asymmetric C1, when the imine fragment derives from a particular α-amino aldehyde (Garner's aldehyde). According to our computational model, the sterecontrol can stem from the different steps present in the proposed mechanism. If the chirality is induced from the carbon atom contiguous to the iminic nitrogen atom, the trans stereocontrol is determined by the preferential axial disposition of the susbtituent at the chiral methine carbon in the first transition state of the reaction. In contrast, when a chiral aldehyde is used as chiral template, the stereocontrol is dictated by the preferential anti disposition between the new σ bond

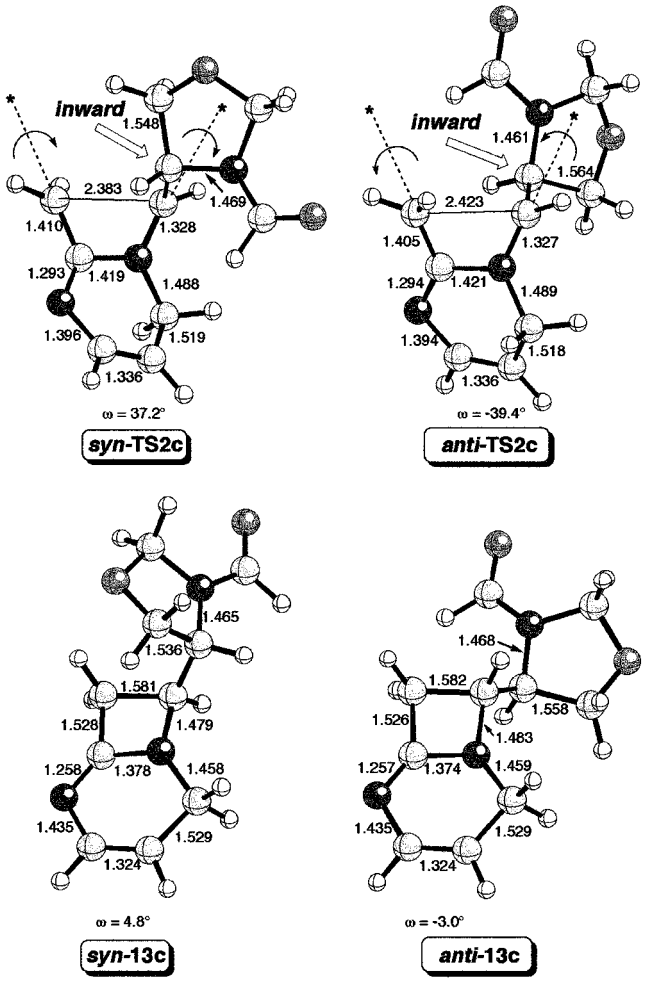

Figure 7. Main geometric features of the stationary points *syn*-**TS2c**, *anti*-**TS2c**, *syn*-**13c**, and *anti*-1**3c** found in the second step of the reaction of **12c** to form *syn*- and *anti*-**13c** (see Scheme 7), computed in the gas phase. See Figure 1 caption for additional details.

being formed and the C−X σ bond present in the reactant, X being an electronegative atom. A high stereocontrol is predicted in this latter case, the syn cycloadduct being the sole isomer formed.

Experimental Section

For general experimental information see ref 7.

Materials. 2-Azidobenzylamine,[29] 1-(*o*-azidophenyl)ethylamine,[13] trimethylsilyl ketene,[30] and diphenylketene[31] were prepared following previously reported procedures. *N*-(2-Azidobenzyl)imines **5** were obtained by standard procedures (Scheme 1, methods A[9] and B[10]).

Preparation of 2-Azido-α-phenylbenzylamine (4b). A solution of $NaNO_2$ (2.07 g, 30 mmol) in H_2O (50 mL) was added dropwise to an ice-cooled solution of 2-amino-α-phenylbenzyl alcohol (3.98 g, 20 mmol) in 6 N HCl (200 mL). The reaction mixture was stirred at 0 °C for 30 min, and then a solution of NaN_3 (1.95 g, 30 mmol) in H_2O (50 mL) was added. After 4 h at room temperature, the reaction mixture was extracted with dichloromethane (3 × 100 mL), and the extracts were dried over $MgSO_4$. The solvent was removed under reduced pressure,

(29) Smith, P. A. S.; Budde, G. F.; Shang-Shing, P. C. *J. Org. Chem.* **1985**, *50*, 2062.
(30) Valenti, E.; Pericás, M. A.; Serratosa, F. *J. Org. Chem.* **1990**, *55*, 395.
(31) Taylor, E. C.; McKillop, A.; Hawks, G. H. *Org. Synth.* **1973**, *52*, 36.

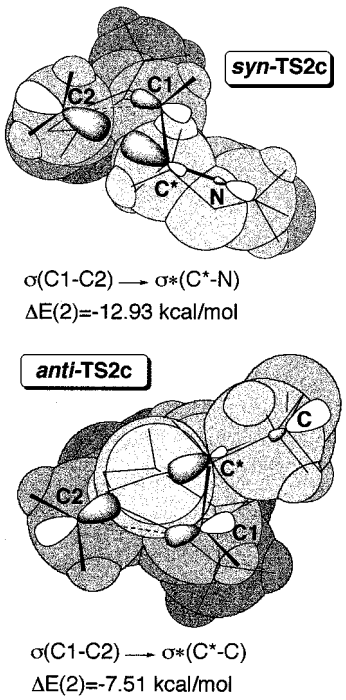

Figure 8. B3LYP/6-31G* second-order perturbational energies (Δ*E*(2)) in *syn*- and *anti*-**TS2c**. The HF/3-21G fully optimized geometries of both transition structures are represented by means of the space-filling model, to enphasize the steric interactions between the forming ring and the chiral oxazolidine moiety.

and the resulting material was purified by column chromatography (silica gel; hexanes/diethyl ether 7:3) to give **2-azido-α-phenylbenzyl alcohol** (60%).

Diethyl azodicarboxylate (3.48 g, 20 mmol) was added at 0 °C to a solution of triphenylphosphane (5.24 g, 20 mmol) in 50 mL of dry tetrahydrofuran. The mixture was stirred for 30 min at that temperature, and then 2-azido-α-phenylbenzyl alcohol (3.38 g, 15 mmol) and phthalimide (2.94 g, 20 mmol) were added. The mixture was stirred 1 h at 0 °C and 24 h at room temperature. The solvent was removed, and the residue was chromatographed (silica gel; hexanes/ethyl acetate 4:1) to obtain ***N*-(2-azido-α-phenylbenzyl)phthalimide** (75%).

Hydrazine hydrate (7.5 equiv) was added to a solution of *N*-(2-azido-α-phenylbenzyl)phthalimide (3.54 g, 10 mmol) in 100 mL of tetrahydrofuran and 16 mL of ethanol. After 16 h at room temperature, the suspension was heated at reflux temperature for 8 h. After cooling, the mixture was filtered, the solid was washed with tetrahydrofuran, and the solvent was removed from the filtrate. The resulting material was purified by column chromatography (silica gel; ethyl acetate/methanol 1:1) to afford **2-azido-α-phenylbenzylamine** (**4b**): yield 91%; colorless oil; IR (Nujol) 3379, 3292, 2117, 1294 cm^{-1}; ^1H NMR ($CDCl_3$) δ 1.77 (br s, 2 H), 5.45 (s, 1 H), 7.12−7.44 (m, 9 H); ^{13}C NMR ($CDCl_3$) δ 54.21, 118.28, 125.09, 127.00, 127.06, 128.14, 128.28, 128.43, 136.86 (s), 137.33 (s), 144.45 (s); mass spectrum *m*/*z* (relative intensity) 224 (M^+, 43), 196 (100). Anal. Calcd for $C_{13}H_{12}N_4$: C, 69.62; H, 5.39; N, 24.98. Found: C, 69.50; H, 5.09; N, 25.41.

General Procedure for the Preparation of Azeto[2,1-*b*]quinazolines 8, 9, and 11. Trimethylphosphane (3 mmol, 1 M toluene solution) was added to a solution of the corresponding azidoimine (3 mmol) in dry toluene (15 mL), and the reaction mixture was stirred at room temperature until the evolution of nitrogen ceased (15−30 min). Then, diphenylketene or trimethylsilylketene (3 mmol) was added, and the reaction mixture was stirred at room temperature or at reflux temperature, respectively, until the ketenimine band around 2000 cm^{-1} was not observed by IR spectroscopy (1−12 h). The solvent was removed under reduced pressure, and the resulting material was chromatographed on a silica gel column, with hexanes/ethyl acetate as eluent.

***trans*-2,2-Diphenyl-8-methyl-1-(4-nitrophenyl)-1,2-dihydroazeto[2,1-*b*]quinazoline (*trans*-8a):** yield 82%; mp 172−173 °C; colorless prisms (diethyl ether); IR (Nujol) 1669, 1519, 1343 cm^{-1}; ^1H NMR ($CDCl_3$) δ 1.42 (d, 3 H, J = 6.2 Hz), 4.73 (q, 1 H, J = 6.2 Hz), 5.86 (s, 1 H), 6.95−7.11 (m, 7 H), 7.24−7.44 (m, 7 H), 7.71 (d, 2 H, J = 8.7 Hz), 8.02 (d, 2 H, J = 8.7 Hz); ^{13}C NMR ($CDCl_3$) δ 21.66, 48.95, 69.28, 69.63 (s), 123.37, 124.84, 125.58, 126.71 (s), 126.80, 127.16, 127.63, 127.70, 128.03, 128.25, 128.40, 128.56, 128.78, 137.07 (s), 140.19 (s), 142.11 (s), 142.93 (s), 147.53 (s), 163.61 (s); mass spectrum *m*/*z* (relative intensity) 445 (M^+, 43), 165 (100). Anal. Calcd for $C_{29}H_{23}N_3O_2$: C, 78.18; H, 5.20; N, 9.43. Found: C, 78.41; H, 5.09; N, 9.25.

***trans*-1-Isopropyl-2,2,8-triphenyl-1,2-dihydroazeto[2,1-*b*] quinazoline (*trans*-8k):** yield 66%; mp 231 °C; white prisms (diethyl ether); IR (Nujol) 1669, 1594, 1564 cm^{-1}; ^1H NMR ($CDCl_3$) δ 0.61 (d, 3 H, J = 6.5 Hz), 0.95 (d, 3 H, J = 6.5 Hz), 1.69−1.79 (m, 1 H), 3.92 (d, 1 H, J = 9.9 Hz), 5.63 (s, 1 H), 6.82 (dd, 1 H, J = 7.5, 1.2 Hz), 6.93 (ddd, 1 H, J = 7.5, 7.2, 1.5 Hz), 7.05−7.39 (m, 15 H), 7.58−7.61 (m, 2 H); ^{13}C NMR ($CDCl_3$) δ 19.22, 20.42, 30.23, 61.10, 65.71 (s), 73.21, 124.58, 125.73, 126.15 (s), 127.25, 127.29, 128.01, 128.07, 128.20,

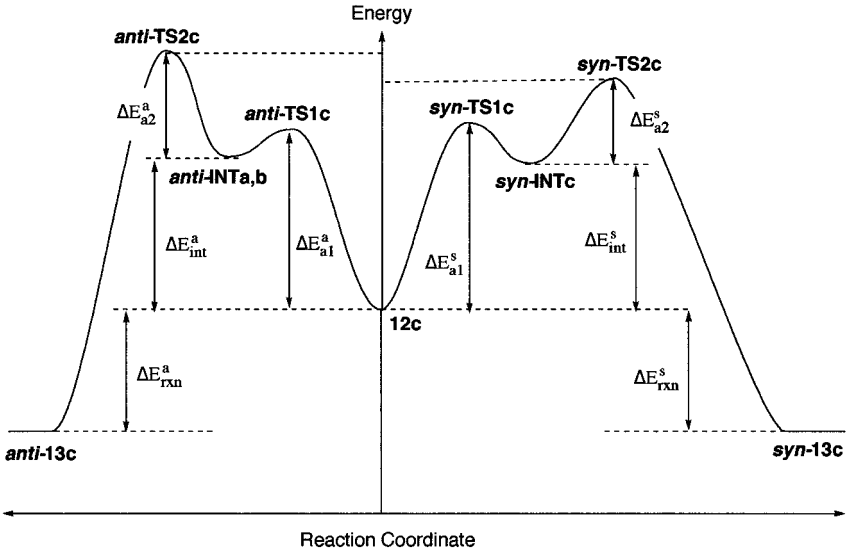

Figure 9. Reaction profile found for the **12c** → *syn*-/*anti*-**13c** transformation.

128.37, 128.47, 128.85, 129.21, 129.24, 139.16 (s), 139.78 (s), 141.44 (s), 141.97 (s), 156.29 (s), one methine carbon was not observed; mass spectrum *m*/*z* (relative intensity) 428 (M^+, 63), 385 (100). Anal. Calcd for $C_{31}H_{28}N_2$: C, 86.88; H, 6.58; N, 6.54. Found: C, 86.65; H, 6.73; N, 6.62.

***trans*-8-Methyl-1-(4-nitrophenyl)-1,2-dihydroazeto[2,1-*b*] quinazoline (*trans*-9a)**: yield 62%; mp 155−156 °C; colorless prisms (diethyl ether); IR (Nujol) 1663, 1596, 1520, 1349 cm^{-1}; ^1H NMR ($CDCl_3$) δ 1.44 (d, 3 H, J = 6.5 Hz), 3.01 (dd, 1 H, J = 14.9, 2.8 Hz), 3.63 (dd, 1 H, J = 14.9, 5.6 Hz), 4.68 (q, 1 H, J = 6.5 Hz), 5.20 (dd, 1 H, J = 5.6, 2.8 Hz), 6.95 (d, 1 H, J = 7.8 Hz), 7.02−7.11 (m, 2H), 7.21 (td, 1 H, J = 7.8, 1.5 Hz), 7.60 (d, 2 H, J = 8.7 Hz), 8.26 (d, 2 H, J = 8.7 Hz); ^{13}C NMR ($CDCl_3$) δ 21.47, 41.61, 49.22, 56.97, 124.24, 124.62, 124.81, 126.68, 126.96, 128.50, 141.80 (s), 145.72 (s), 147.94 (s), 159.59 (s), one quaternary carbon was not observed; mass spectrum *m*/*z* (relative intensity) 293 (M^+, 11), 278 (100). Anal. Calcd for $C_{17}H_{15}N_3O_2$: C, 69.61; H, 5.15; N, 14.32. Found: C, 69.88; H, 5.01; N, 14.37.

Azeto[2,1-*b*]quinazoline 11: yield 42%; mp 186−187 °C; colorless prisms (diethyl ether); IR (Nujol) 1691, 1664, 1598 cm^{-1}; ^1H NMR ($CDCl_3$, 328 K) δ 1.44 (s, 9 H), 1.49 (s, 3 H), 1.75 (s, 3 H), 3.55 (dd, 1 H, J = 9.6, 5.1), 3.81 (d, 1 H, J = 9.6 Hz), 3.85 (bs s, 1 H), 4.44 (d, 1 H, J = 12.0 Hz), 4.50 (d, 1 H, J = 9.6 Hz), 4.54 (d, 1 H, J = 12.0 Hz), 6.80 (d, 1 H, J = 7.45 Hz), 6.91−7.01 (m, 1 H), 7.15−7.45 (m, 10 H), 7.64 (d, 2 H, J = 7.1 Hz); mass spectrum *m*/*z* (relative intensity) 509 (M^+, 30), 310 (100); $[\alpha]^{25}_D$ = +176.8 (*c* 1.38, $CHCl_3$). Anal. Calcd for $C_{32}H_{35}N_3O_3$: C, 75.41; H, 6.92; N, 8.24. Found: C, 75.65; H, 6.81; N, 8.03.

Acknowledgment. The work in Murcia was supported by the Dirección General de Enseñanza Superior (Project PB95-1019), Fundación Séneca-CARM (Project PB/2/FS/99), and by Acedesa (a division of Takasago). The work in San Sebastián-Donostia was supported by the Secretaria de Estado, Investigación y Desarrollo (Project PB96-1481) and by the Gobierno Vasco-Eusko Jaurlaritza (Projects EX-1998-126 and PI-1998-116). One of us (F.T.) also thanks the MEC for a fellowship.

Supporting Information Available: Characterization data for products **8b**−**j** and **9b**−**e**, as well as total energies and zero-point vibrational energies of all stationary points of the reactions studied by computational methods. This material is available free of charge via the Internet at http://pub.acs.org.

JO991826Q